Palestine Journal of Mathematics

Vol. 11(2), (2022) , 604–616

HEAT TRANSFER AND FLOW OF MHD MICROPOLARNANOFLUID THROUGH THE POROUS WALLS, MAGNETIC FIELDS AND THERMAL RADIATON

A.T. Akinshilo, A. G. Davodi, H. Rezazadeh, G. Sobamowo and Cemil Tunç

Communicated by Ayman Badawi

MSC 2020 Classifications: Primary 76D07, 76W05, 80A20.

Keywords and phrases: Non-linear ordinary differential equations, Porous wall channel, Thermal radiation, Homotopy Perturbation Method (HPM); MHD

Abstract The analytical study of heat transfer and on the other hand flow of MHD micro-polar nano fluid, which is affected by thermal radiation in a magneto porous wall channel, is presented. Equations governing the momentum and energy mechanics are transformed to differentials of nonlinear ordinary equations with the appropriate boundary conditions adopting the similarity transformation technique. The differentials of non-linear ordinary equations (ODE) are solved analytically using HPM method. Several significant parameters such as the nano fluid concentration, the micro-polar parameter, the radiation parameter on the temperature and velocity profiles and magnetic parameter are investigated. Moreover, figures illustrate what the actual Nusselt number is.

1 Introduction

In the bid to describe the fluid with rotating micro-particles, the theory of micro-polar fluid was developed from past decades. The fluid with both the components rotational motion and the macroscopic velocity field are called micro-polar fluid. These fluids such as blood flows, bubbly liquids and Ferro-fluids consist of components that are suspended in the fluid especially viscous fluid. In addition, these fluids have many applications in industrial products such as colloidal expansions, polymer solutions, biological structures and lubricant fluids.

Firstly, Eringen [1] formulated the theory of micro-polar fluids in 1966 and presented boundary conditions and governing equations. These equations were solved by considering the thermodynamic limitations. The blood flow can be formulated by using this model as micro rotations and these types of fluids [2]. Beside the numerus researches in the field of micro-polar fluids, there is need of some needs in this field [3, 4]. Flow of these fluids, where flat plate is considered, was studied in [5], Rees and Bassom [6]. There are several researches in these field which studied this theory and addressed several questions [7–12].

In terms of solving nonlinear differential equations governing on natural phenomena, several analytical methods were developed in last decades [13-20]. The coupled nonlinear ODE was solved utilizing HPM [21-26]. The efficient parameters in these phenomena are Peclet number, the Reynolds number and angular velocity which have significant impact on stream function and negligible impact on temperature and concentration fields.

Problem of MHD, where natural convection layer on the boundary flow is considered near the vertical surface, was investigated in [27]. He transformed governing equation to dimensionless form by applying stream function formulations and solved it numerically. He showed the micro-polar and the magnetic parameters do not affect heat transfer. Srinivasacharya et al. [28] investigated the heat transfer and the entropy generation of micro-polar fluid movement in a magnetic annulus field. The equations were derived by utilizing Chebyshev spectral collocation. He showed that the inner cylinder has the highest entropy generation and the outer cylinder has the minimum entropy generation. The numerical investigation on the non-uniform heat effects on convective MHD non-porous flow was studied by Mabood et al. [29]. They revealed the velocity profile reduces as the magnetic factor increases. They also proved that in this case concentration and the temperature rise.

There are also numerous investigations on heat transfer effect parameters in diverse aspects. The thermal conductivity in the nano fluid is more in comparison with the normal fluid because of the metallic nanoparticles which are suspended in the fluid. Ellahi et al. [30] studied the particle shape impacts on the mixed convection nano fluid flow over the porous medium wedge. The authors in [31] studied the force heat transfer and laminar nano fluid flow through a wavy channel and the impact of Nusselt number on the Reynolds number was shown in their study. Ellahi et al. [32] examined the same problem as [31] in the vicinity of a mixed convection and a stagnation point flow in the two-dimensional coordinate system. They showed the radius of gyration, chemical dimensions and volume friction increase when the temperature of nano fluid elevate up and the nano fluid velocity decrease by increasing fractal dimensions and the concentration of particle volume fraction. Moreover, numerous publications investigated the effect of using nanoparticles since recent years [32-40] and see also for some works in [41-45].

2 Problem description

In this section, two-dimensional laminar fluid flowing steadily in a porous wall channel with magnetic impact is considered. It is assumed that the input speed and output speed of fluid are the same v0, the temperature of bottom wall is T_1, and the temperature of top wall is T_2. As it can be seen in Figure 1, channel wall's surface is perpendicular to y-axis, or more precisely at $y = \pm h$. We assume that the nano fluid studied in this problem is Newtonian and more importantly compressible. Moreover, sticking velocity is assumed during fluid flow and the nano mix is in thermal equilibrium, i.e., there is thermal equilibrium between the nanoparticles and base fluid.

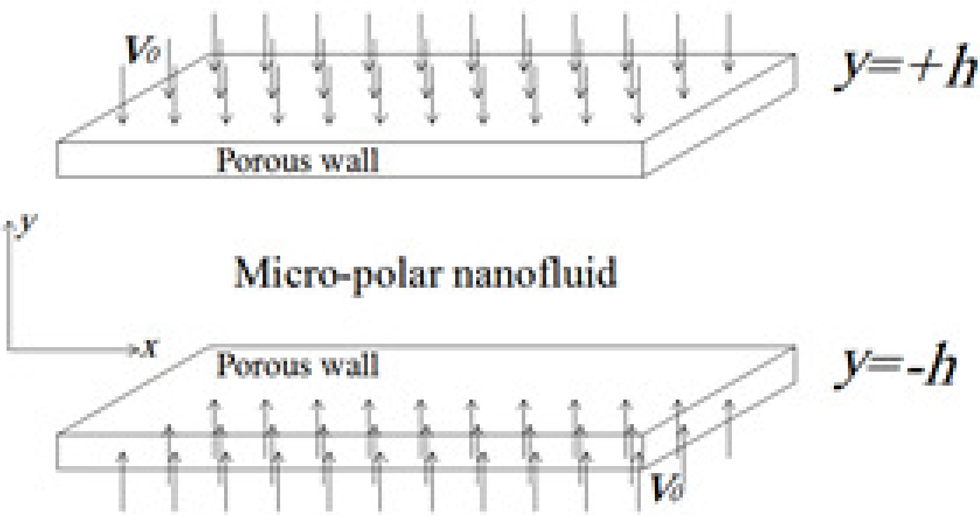

Figure 1. Physical model of laminarmicro-polar nano fluid flow

The general form of the basic equations for energy and conservative momentums is reformulated as follows:

$$\frac{\partial u}{\partial x} + \frac{\partial v}{\partial y} = 0, \tag{2.1}$$

$$\rho_{nf}\left(u\frac{\partial u}{\partial x} + v\frac{\partial u}{\partial y}\right) = -\frac{\partial p}{\partial x} + (\mu_{nf} + k)\left(\frac{\partial^2 u}{\partial x^2} + \frac{\partial^2 u}{\partial y^2}\right) + k\frac{\partial N}{\partial y} - \sigma_f B_0^2 u, \tag{2.2}$$

$$\rho_{nf}\left(u\frac{\partial v}{\partial x} + v\frac{\partial v}{\partial y}\right) = -\frac{\partial p}{\partial x} + (\mu_{nf} + k)\left(\frac{\partial^2 v}{\partial x^2} + \frac{\partial^2 v}{\partial y^2}\right) - k\frac{\partial N}{\partial x}, \tag{2.3}$$

$$\rho_{nf} j\left(u\frac{\partial N}{\partial x} + v\frac{\partial N}{\partial y}\right) = -k\left(2N + \frac{\partial u}{\partial y} - \frac{\partial v}{\partial x}\right) + \gamma_{nf}\left(\frac{\partial^2 N}{\partial x^2} + \frac{\partial^2 N}{\partial y^2}\right), \tag{2.4}$$

$$u\frac{\partial T}{\partial x}+v\frac{\partial T}{\partial y}=\frac{k_{nf}}{(\rho C_p)_{nf}}\left(\frac{\partial^2 T}{\partial x^2}+\frac{\partial^2 T}{\partial y^2}\right)-\frac{1}{(\rho C_p)_{nf}}\frac{\partial q_{rad.}}{\partial y}, \tag{2.5}$$

where $P, B_0, u, v, T, \sigma_f, N, k, j, q_{rad}$ and γ_{nf} are the pressure, the magnetic field, the velocity in the x direction velocity, y direction velocity, the temperature, the electric conductivity of the fluid, the micro-rotation velocity, the viscosity of vortex, the spin-gradient viscosity, the radiative heat flux and the micro-inertia $\gamma_{nf} = -(\mu_{nf} - +\frac{k}{2})j$, respectively. Rosseland approximation is considered for radiation:

$$q_{rad} = -\left(4\sigma^*/3k^*_{nf}\right)\frac{\partial T^4}{\partial y}, \tag{2.6}$$

where σ^* is the Stefan–Boltzmann constant, while the constant k^*_{nf} is the coefficient of absorption of the nano fluid. More so, flow temperature variation is a function of distance. Therefore T^4 is expanded adopting the Taylor series. By ignoring higher order terms, we expand T^4 about T^∞:

$$T^4 \cong 4T^3_\infty T - 3T^4_\infty. \tag{2.7}$$

Eq. (5) is rewritten:

$$u\frac{\partial T}{\partial x}+v\frac{\partial T}{\partial y}=\frac{k_{nf}}{(\rho C_p)_{nf}}\left(\frac{\partial^2 T}{\partial x^2}+\frac{\partial^2 T}{\partial y^2}\right)+\frac{16\sigma^* T^3_\infty}{3k^*_{nf}(\rho C_p)_{nf}}\frac{\partial^2 T}{\partial y^2}, \tag{2.8}$$

$$\begin{aligned}
\rho_{nf} &= (1-\phi)\,\rho_f + \phi\rho_s,\\
(\rho C_p)_{nf} &= (1-\phi)\,(\rho C_p)_f + \phi(\rho C_p)_s,\\
\mu_{nf} &= \frac{\mu_f}{(1-\phi)^{2.5}},
\end{aligned} \tag{2.9}$$

$$\frac{k_{nf}}{k_f} = \frac{k_s + 2k_f - 2\phi\,(k_f - k_s)}{k_s + 2k_f + 2\phi\,(k_f - k_s)}.$$

Note that ρ_{nf}, μ_{nf}, are the density effective and the dynamic viscosity effective, while $(\rho Cp)_{nf}$ and k_{nf} are the capacitance of heat and the nano fluid thermal conductivity. Some of these parameters are presented for copper and water in Table 1.

	$\rho\,(Kg/m^3)$	$C_p\,(J/KgK)$	$K\,(w/mk)$
Copper (Cu)	8933	385	401
Water	997.1	4179	0.613

Table 1. The rmophysical properties of nanofluid (see [33])

The boundary conditions for Eq. (8) are given as follows:

$$u = 0, v = -v_0, N = -s\left.\frac{\partial u}{\partial y}\right|_{y=-h} T = T_1, \text{ at } y = -h,$$

$$u = 0, v = v_0, N = -s\left.\frac{\partial u}{\partial y}\right|_{y=+h} T = T_2, \text{ at } y = +h, \tag{2.10}$$

where s demonstrates the microelements' rotational factor close to walls. If $s = 0$, then there is no microelements rotation near the walls and concentrated particle flows is occurred. Weak concentration and the turbulent flow are occurred if $s = 0.5$ and $s = 1$, respectively.The suction and injection are occurred if $v_0 > 0$ and $v_0 < 0$, respectively. The dimensionless parameters are presented as follows:

$$\eta = \frac{y}{h},\ u = -\frac{v_0 x}{h} f'(\eta),\ N = \frac{v_0 x}{h^2} g(\eta),$$
$$v = v_0, f(\eta),\ \theta = (T - T_1)/(T_2 - T_1),\ T_2 = T_1 + Ax. \tag{2.11}$$

From above the coupled system of nonlinear equations, it is achieved by substituting above equations into the equations (1-5) and then removing the pressure gradient:

$$\left(1 + (1-\phi)^{2.5} K\right) f^{iv}) - (1-\phi)^{2.5} K g''$$
$$- \left(1 - \phi + \tfrac{\rho_s}{\rho_f}\phi\right)(1-\phi)^{2.5} R_e (f f''' - f' f'') - (1-\phi)^{2.5} M n f'' = 0, \tag{2.12}$$

$$\left(1 + \frac{(1-\phi)^{2.5}}{2} K\right) g'' + (1-\phi)^{2.5} K (f'' - 2g)$$
$$- \left(1 - \phi + \frac{\rho_s}{\rho_f}\phi\right)(1-\phi)^{2.5} R_e (f g' - g f') = 0, \tag{2.13}$$

$$\theta'' + \left((1-\phi) + \frac{(\rho C_p)_s}{(\rho C_p)_f}\phi\right)\left(\frac{3N}{3N+4}\right)\frac{k_f}{k_{nf}} P_r R_e (f'\theta - f\theta') = 0. \tag{2.14}$$

The boundary condition is presented by:

$$\begin{aligned} &f(-1) = -1,\ f'(-1) = 0,\ f(+1) = 1,\ f'(+1) = 0, \\ &g(-1) = 0,\ g(+1) = 0, \\ &\theta(-1) = 0,\ \theta(+1) = 1. \end{aligned} \tag{2.15}$$

Where K and P_r are the micropolar parameter and Prandtl number, while R_e, N and M_n are the Reynolds number, the radiation parameter and the magnetic parameter, respectively. These numbers can be presented as follows:

$$\begin{aligned} &R_e = \rho_f v_0 h/\mu_f,\ P_r = \mu_f C_{p,f}/k_f,\ Nr = k_{nf} k^*_{nf}/4\sigma^* T^3_\infty, \\ &Mn = \sigma_f B_0^2 h^2/\mu_f,\ K = k/\mu_f,\ j = h^2. \end{aligned} \tag{2.16}$$

The suction and the injection will be occurred if $R_e > 0$ and $Re < 0$, respectively. The Nusselt number (Nu^*) is another considerable parameter of this study:

$$Nu^* = -\left(\frac{h}{k_f (T_2 - T_1)}\right)\left(k_{nf} + \frac{16\sigma^* T^3_\infty}{3k^*_{nf}}\right)\left.\frac{\partial T}{\partial y}\right|_{y=-h}. \tag{2.17}$$

From Equations (9) and (11), we can write:

$$Nu = \left|\frac{k_{nf}}{k_f}\left(\frac{3Nr + 4}{3Nr}\right)\theta'(-1)\right|. \tag{2.18}$$

3 Analytical solution of problem

In this section the transport and heat transport of micropolar fluid through penetrable wall considering thermal radiation and magnetic field is studied utilizing HPM. The principles and fundamentals of the HPM, an approximate method of analytical solution has been extensively described by J.H. He [21-22]. The HPM been an analytical method with fast rate of convergence, coupled with procedural stability is the selected method adopted to generate solution to the system of coupled higher order differentials. Therefore, constructing the homotopy the governing equations Eqs. (12)- (14) are expressed as follows:

$$H_1(p,\eta) = (1-p)\left[\frac{d^4 f}{\partial\eta^4}\right] + p\left[\begin{array}{c}\frac{d^4 f}{d\eta^4} - (1-\phi)^{2.5}K\frac{d^2 g}{d\eta^2} - \left(1-\phi+\frac{\rho s}{\rho f}\phi\right)(1-\phi)^{2.5}\,\mathrm{Re}\left(f\frac{d^3 f}{d\eta^3} - f\frac{d^2 f}{d\eta^2}\right)\\ -(1-\phi)^{2.5}M^2\frac{d^2 f}{d\eta^2}\end{array}\right] / \left(1+(1-\phi)^{2.5}K\right) = 0, \tag{3.1}$$

$$H_2(p,\eta) = (1-p)\left[\frac{d^2 g}{d\eta^2}\right] + p\left[\begin{array}{c}\frac{d^2 g}{d\eta^2} - (1-\phi)^{2.5}K\left(\frac{d^2 f}{d\eta^2} - 2g\right) - \left(1-\phi+\frac{\rho s}{\rho f}\phi\right)\\ (1-\phi)^{2.5}\,\mathrm{Re}\left(f\frac{dg}{d\eta} - g\frac{df}{d\eta}\right)\end{array}\right] / \left(1+\frac{(1-\phi)^{2.5}}{2}K\right) = 0, \tag{3.2}$$

$$H_2(p,\eta) = (1-p)\left[\frac{d^2\theta}{d\eta^2}\right] + p\left[\frac{d^2\theta}{d\eta^2} + \left((1-\phi)+\frac{(\rho C_p)_s}{(\rho C_p)_f}\phi\right)\left(\frac{3N}{3N+4}\right)\frac{k_f}{k_{nf}}\,\mathrm{Pr}\,\mathrm{Re}\left(\frac{df}{d\eta}\theta - f\frac{d\theta}{d\eta}\right)\right] = 0. \tag{3.3}$$

Note that, by taking power series of velocity and similarly temperature fields, we obtain the following equations:

$$f = P^0 f_0 + P^1 f_1 + P^2 f_2 + ..., \tag{3.4}$$

$$g = P^0 g_0 + P^1 g_1 + P^2 g_2 + ..., \tag{3.5}$$

$$\theta = P^0\theta_0 + P^1\theta_1 + P^2\theta_2 + ... \tag{3.6}$$

Substituting Eq. (22) into (19) and selecting at the various order yields

$$p^0 : \frac{d^4 f_0}{d\eta^4}, \tag{3.7}$$

$$p^1 : \left[\begin{array}{c}\frac{d^4 f_1}{d\eta^4} - (1-\phi)^{2.5}K\frac{d^2 g_0}{d\eta^2} - \left(1-\phi+\frac{\rho s}{\rho f}\phi\right)(1-\phi)^{2.5}\,\mathrm{Re}\left(f_0\frac{d^3 f_0}{d\eta^3} - f_0\frac{d^2 f_0}{d\eta^2}\right)\\ -(1-\phi)^{2.5}M^2\frac{d^2 f_0}{d\eta^2}\end{array}\right] / \left(1+(1-\phi)^{2.5}K\right), \tag{3.8}$$

$$p^2 : \left[\begin{array}{c}\frac{d^4 f_2}{d\eta^4} - (1-\phi)^{2.5}K\frac{d^2 g_1}{d\eta^2} - \left(1-\phi+\frac{\rho s}{\rho f}\phi\right)(1-\phi)^{2.5}\,\mathrm{Re}\, f_0\frac{d^3 f_1}{d\eta^3}\\ +\left(1-\phi+\frac{\rho s}{\rho f}\phi\right)(1-\phi)^{2.5}\,\mathrm{Re}\, f_0\frac{d^2 f_1}{d\eta^2} - (1-\phi)^{2.5}M\frac{d^2 f_1}{d\eta^2}\end{array}\right] / \left(1+(1-\phi)^{2.5}K\right). \tag{3.9}$$

Similar to above, by utilizing (23) in (20), we have

$$p^0 : \frac{d^2 g}{d\eta^2}, \tag{3.10}$$

$$p^1 : \left[\begin{array}{c} \frac{d^2 g_1}{d\eta^2} - (1-\phi)^{2.5} K \left(\frac{d^2 f_0}{d\eta^2} - 2g_0 \right) - \left(1 - \phi + \frac{\rho s}{\rho f} \phi \right) \\ (1-\phi)^{2.5} \operatorname{Re} \left(f_0 \frac{dg_0}{d\eta} - g_0 \frac{df_0}{d\eta} \right) \end{array} \right]$$
$$/ \left(1 + \frac{(1-\phi)^{2.5}}{2} K \right). \tag{3.11}$$

Similarly, from (24) and (21), we conclude that

$$p^0 : \frac{d^2\theta_0}{d\eta^2}, \tag{3.12}$$

$$p^1 : \frac{d^2\theta}{d\eta^2} + \left((1-\phi) + \frac{(\rho C_p)_s}{(\rho C_p)_f} \phi \right) \left(\frac{3N}{3N+4} \right) \frac{k_f}{k_{nf}} \operatorname{Pr} \operatorname{Re} \left(\frac{df}{d\eta} \theta - f \frac{d\theta}{d\eta} \right), \tag{3.13}$$

$$p^2 : \frac{d^2\theta_2}{d\eta^2} + \left((1-\phi) + \frac{(\rho C_p)_s}{(\rho C_p)_f} \phi \right) \left(\frac{3N}{3N+4} \right) \frac{k_f}{k_{nf}} \operatorname{Pr} \operatorname{Re} \left(\frac{df_0}{d\eta} \theta_1 - f_0 \frac{d\theta_1}{d\eta} \right). \tag{3.14}$$

Leading order boundary condition can be written as follows:

$$f_0(-1) = -1, \frac{df_0}{d\eta}(-1) = 0, f_0(1) = 1, \frac{df_0}{d\eta}(1) = 0. \tag{3.15}$$

Applying (33) to (25), we derive f_0 as follows:

$$f_0 = \frac{3\eta}{2} - \frac{\eta^3}{2}. \tag{3.16}$$

Similarly, for the function $g(.)$, we have

$$g(-1) = 0, g(1) = 0. \tag{3.17}$$

Similar to (34), we derive g_0 as follows:

$$g_0 = \frac{\eta}{2} + \frac{1}{2}. \tag{3.18}$$

Similarly, for the function θ , we have

$$\theta(-1) = 0, \theta(1) = 1, \tag{3.19}$$

$$\theta_0 = \frac{\eta}{2} + \frac{1}{2}. \tag{3.20}$$

The boundary condition is presented as

$$f_1(-1) = -1, \frac{df_1}{d\eta}(-1) = 0, f_1(1) = 1, \frac{df_1}{d\eta}(1) = 0. \tag{3.21}$$

Utilizing (39) in (26), we conclude the following equation:

$$f_1 = \Big(-(\operatorname{Re}/140 - Re\phi/140)/(8K((1-\phi)^{2.5} + 8\Big) - (\operatorname{Re}\phi\rho s)/(1120\rho f(K(1-\phi)^{2.5} + 7)$$
$$+ (\operatorname{Re}\phi\rho s)/(560\rho f(K(1-\phi)^{2.5} + 1)))\eta^7 + (((3\operatorname{Re})/40 - (3Re\phi)/40)/(6K(1-\phi)^{2.5} + 6)$$
$$+ (\operatorname{Re}\phi\rho s)/(80\rho f(K(1-\phi)^{2.5} + 1)))\eta^6 + (-((3\operatorname{Re})/16 - (3\operatorname{Re}\phi)/16$$
$$+ (M(1-\phi)^{2.5}/8)(5K(1-\phi)^{2.5} + 5) + ... \tag{3.22}$$

Note that, the boundary condition here is represented as

$$g_1(-1) = 0, g_1(1) = 0. \tag{3.23}$$

Using (41) in (29), we obtain

$$\begin{aligned}
g_1 &= \eta^4[((\mathrm{Re}\,(1-\phi)^{2.5}/2(\mathrm{Re}\,\phi(1-\phi)^{2.5})/2)/(4(K(1-\phi)^{2.5}+2))\\
&+ (\mathrm{Re}\,\phi\rho s(1-\phi)^{2.5})/(8\rho f(K(1-\phi)^{2.5}+2)))\\
&+ \eta^5(((\mathrm{Re}\,(1-\phi)^{2.5})/4-(\mathrm{Re}\,\phi(1-\phi)^{2.5})/4)/(5(K(1-\phi)^{2.5}+2))\\
&+ (\mathrm{Re}\,\phi\rho s(1-\phi)^{2.5})/(20\rho f(K(1-\phi)^{2.5}+2))\\
&+ \eta^2((2K(1-\phi)^{2.5}-(3\,\mathrm{Re}\,(1-\phi)^{2.5}))/2\\
&+ (3\,\mathrm{Re}\,\phi\rho s(1-\phi)^{2.5})/(4\rho f(K(1-\phi)^{2.5}+2)))-((\mathrm{Re}\,(1-\phi)^{2.5})/2+....
\end{aligned} \tag{3.24}$$

Similar to above, we have

$$\theta_1(-1)=0, \theta_1(1)=1, \tag{3.25}$$

$$\begin{aligned}
\theta_1 &= (3N\,\mathrm{Pr}\,\mathrm{Re}\,k_f(\rho C_f-\rho C_f\phi+\rho C_s\phi)\eta^5)/(40k_{nf}\rho C_f(3N+4))\\
&+ (3N\,\mathrm{Pr}\,\mathrm{Re}\,k_f(\rho C_f-\rho C_f\phi+\rho C_s\phi)\eta^4/(16k_{nf}\rho C_f(3N+4)\\
&- (9N\,\mathrm{Pr}\,\mathrm{Re}\,k_f\rho C_f-\rho C_f\phi+\rho C_s\phi)\eta^2/(8k_{nf}\rho C_f(3N+4))\\
&+ (1/2+(3N\,\mathrm{Pr}\,\mathrm{Re}\,k_f(\rho C_f-\rho C_f\phi+\rho C_s\phi))/(40k_{nf}\rho C_f(3N+4)))\eta+....
\end{aligned} \tag{3.26}$$

The coefficient of p^2 in $f(\eta)$, $g(\eta)$ and $\theta(\eta)$ in Eqs.(27), (29) and (32) are too heavy to write in this article. Therefore, we present and show these functions graphically in the results and the following table. Therefore, flow and heat transfer are presented as follows:

$$f(\eta) = f_0(\eta) + f_1(\eta) + f_2(\eta), \tag{3.27}$$

$$g(\eta) = g_0(\eta) + g_1(\eta) + g_2(\eta), \tag{3.28}$$

$$\theta(\eta) = \theta_0(\eta) + \theta_1(\eta) + \theta_2(\eta). \tag{3.29}$$

These problems were solved numerically using finite element numerical method (FEM) by Takhar et al. [34] and approximately using the Duan-Rach approach (DRA) by Ganji et al [35]. We validate our result with these methods. There is a precise agreement as those have been showed in Tables 2 and 3.

R	FEM	HPM	FEM	HPM	FEM	HPM	FEM	HPM
	Re=-5	Re=-5	Re=-1	Re=-1	Re=1	Re=1	Re=5	Re=5
5	3.12232	3.1231	3.15858	3.1487	3.17854	3.1673	3.22218	3.2163
10	4.81237	4.8034	4.86364	4.8372	4.89095	4.8756	4.94897	4.9352

Table 2. Comparison of values for $g'(1)$ with the numerical result

R	DRA	HPM	DRA	HPM	DRA	HPM	DRA	HPM
	Re=-5	Re=-5	Re=-1	Re=-1	Re=1	Re=1	Re=5	Re=5
5	3.126127	3.1231	3.15933	3.1487	3.17779	3.1673	3.218511	3.2163
10	4.817155	4.8034	4.86459	4.8372	4.88999	4.8756	4.944212	4.9352

Table 3. Comparison of values for $g'(1)$ with the Duan-Rach approach (DRA)

4 Results and Discussion

Here, the influences of several characteristics (magnetic parameter (Mn), nanoparticle concentration, Reynold parameter and micro-polar parameter) on the velocity profile, micro rotation profile and thermal profile are presented.

In Figure 2, the impacts of the micro-polar parameter on the flow and micro rotation distribution are illustrated. With numeric enhancement of the micro-polar parameter, the velocity distribution and the momentum boundary layer thickness reduce to $\eta = 0$. For $\eta > 0$, this experience is a reverse trend and the velocity of micro-polar fluid $(K > 0)$ is higher than viscous fluids $(K = 0)$. In addition, from the $\eta = -1$ (the lower plate level) to $\eta = 0$ (middle of the channel), the micro-rotation is unsupported by the micro-elements which are derived from the bottom plate, so the micro-rotation distribution is improved by growing the micro-polar parameter. On the other hand, from the middle of the channel to upper plate ($\eta = 0$ to $\eta = 1$), when the micro-polar parameter increases, micro-rotation profile is reduced. In terms of dominant concentration, the microelements which are near the walls do not able to rotate, so there are no plate's micro-rotation.

The Figure 3 illustrates the influence of magnetic field applied constantly on the flow, micro-rotation and the temperature functions. As presented graphically in Figure 3-a, with the quantitative increase of the magnetic parameter, the velocity distribution near the lower plate is enhanced while near the top plate decreases. In addition, the micro-rotation near the bottom plate has positive value. On the other hand, the opposite rotation occurs near the top plates which means the micro-rotation has negative value near the top plate. In this research, the dominant microelements concentration is assumed which implies there is no micro-rotation of the plates. The increase of magnetic field strength reduces the angular micro-rotation which is illustrated in Figure 3-b. Finally, the temperature distribution and the thickness of the thermal boundary layer are slightly reduced by increasing magnetic field strength, Figure 3.c.

The impact of Reynolds number on the velocity and temperature profiles is illustrated in Figure 4. Figure 4.a shows that by numeric increase of the Reynolds number the velocity distribution close to the bottom plate is increased but it is decreased close the top plate. Figure 4.b reveals that temperature profile and the thickness of thermal boundary layer enhances by increasing the η from -1 to 0, while for η from 0 to 1, those reduce. In addition, the impact of the Reynolds number on temperature profiles in middle of channel is maximum while the Reynolds number has not influence on temperature profiles in vicinity of bottom or top walls.

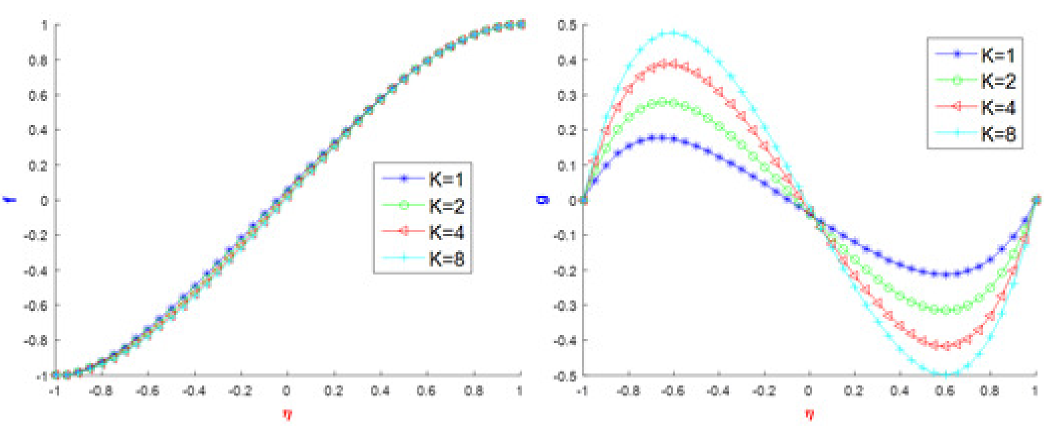

Figure 2. Effect of micro-polar parameter on a: velocity profile and b: on micro rotation profile.

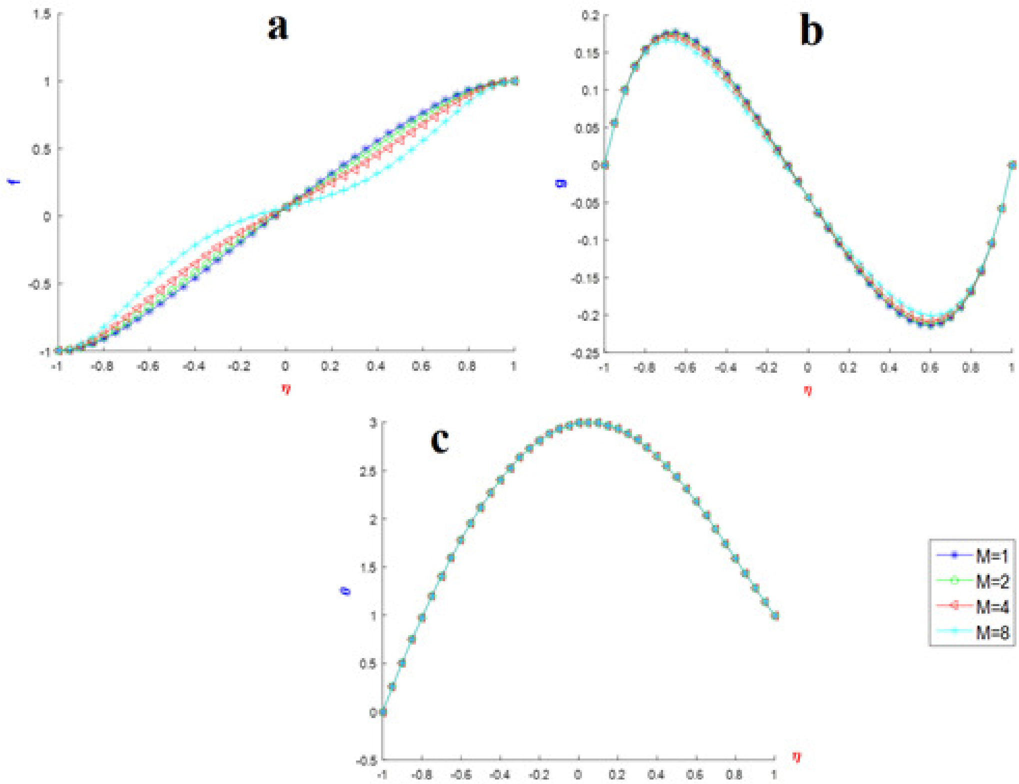

Figure 3. Effect of magnetic parameter on a: velocity profile, b: micro rotation profile and c: thermal profile.

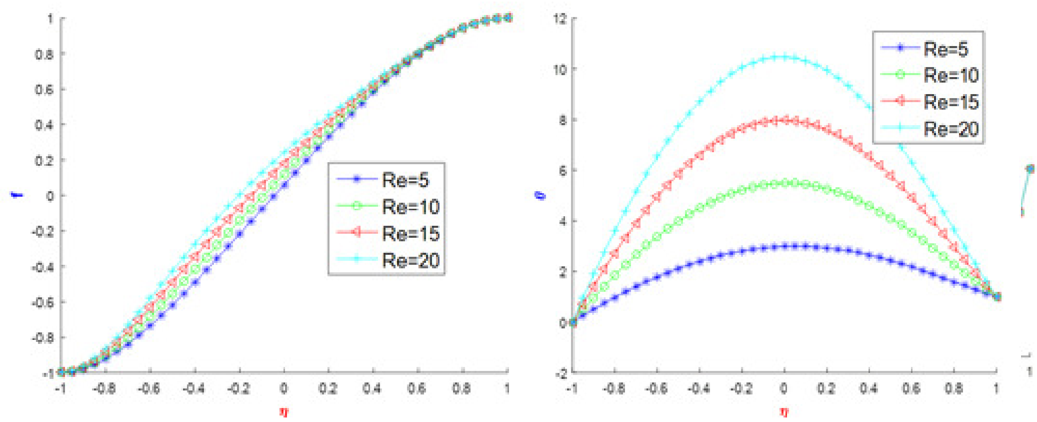

Figure 4. Effect of Reynolds number on a: velocity profile and b: on the thermal profile

In Figure 5, influence of nanoparticle concentration on velocity profile, micro rotation profile and thermal profile are illustrated. Figure 5.a shows, although nanoparticle concentration has not significant impact on the velocity profile, the amount of velocity for higher nanoparticle concentration is greater. In addition, Figure 5.b present from the $\eta = -1$ (the lower plate level) to $\eta 0$ (middle of the channel), the micro-rotation has greater value for higher nanoparticle concentration, while for $\eta = 0$ to $\eta = 1$, it reduces when nanoparticle concentration increases. Finally, from Figure 5.c it can be observed that temperature profile and the thermal boundary layer thickness heighten by increasing the η from -1 to 0, while for η from 0 to 1, those decrease. Moreover, influence of the nanoparticle concentration on temperature profiles in the middle of channel is increased by greater value of nanoparticle concentration.

Finally, in Figure 6 the influence of nanoparticle concentration and micropolar parameter on the Nusselt number are depicted. Figure 6.a shows the Nusselt number is decreased by increasing the nanoparticle concentration from bottom wall to middle of channel while it is inverse for middle of channel to top wall. The Nusselt number is decreased by increasing the micropolar parameter which is presented in Figure 6.b.

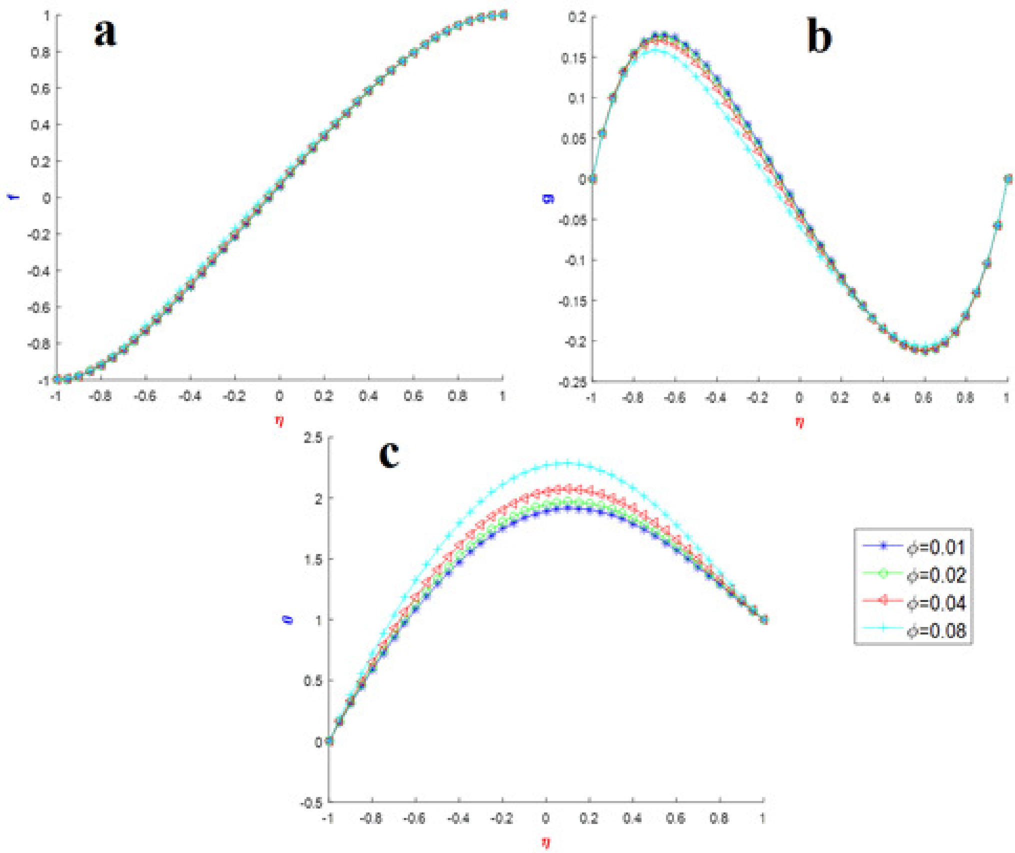

Figure 5. Effect of nanoparticle concentration on a: velocity profile, b: micro rotation profile and c: thermal profile

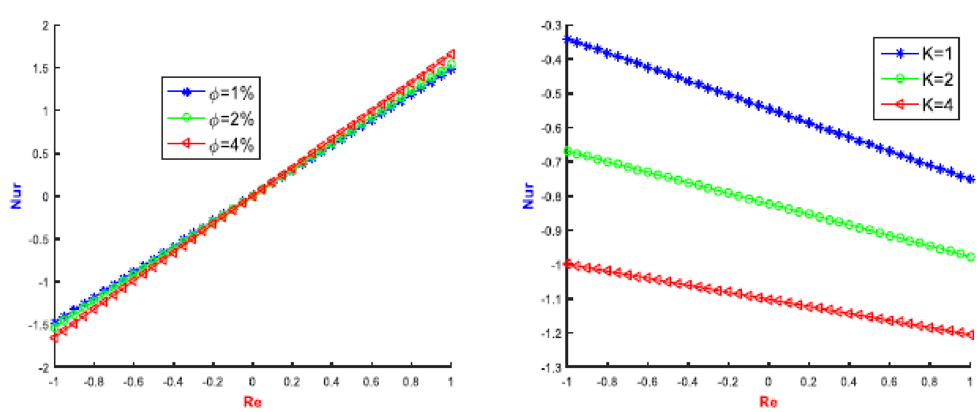

Figure 6. Impact of a: nanoparticle concentration and b: micro polar parameter on Nusselt number

5 Conclusion

This study considers the mass and heat transfer flow of MHD micro-polar Nano-fluid flow through the porous wall channel under the influence of thermal radiation and magnetic field. This was investigated utilizing the homotopy perturbation method. The comparison between HPM method, finite element numerical method and Duan-Rach approach illustrated the precise of our study. The influences of several characteristics (magnetic parameter, nanoparticle concentration, Reynold parameter and micro-polar parameter) on the velocity profile, micro rotation profile and thermal profile were presented. The results showed that when the micro-polar parameter increases, temperature profile rises slightly. Moreover, when the Nusselt number increased, concentration of nanofluid volume and radiation parameter increased.

References

[1] A.C. Eringen, Theory of micropolar fluids. Journal of Mathematics and Mechanics 16 (1966), no.1, 1-18.

[2] A. Mirzaaghaian, D.D. Ganji, Application of differential transformation method in micro polar fluid flow and heat transfer through permeable walls. Alexandria Engineering Journal 55 (2016), no.3, 2183-2191.

[3] R.S. Gorla, J. Eppichs, Heat transfer in micropolar boundary layer flow over a flat plate. Int. J. Eng. Sci. 21 (1983), 791–798.

[4] D.A.S. Rees, A.P. Bassom, The blasius boundary-layer flow of a micropolar fluid. Int. J. Eng. Sci. 34 (1996), 113–124.

[5] M. Esmaeilpour, G Domairry, N Sadoughi, A.G. Davodi, Homotopy analysis method for the heat transfer of a non-Newtonian fluid flow in an axisymmetric channel with a porous wall. Communications in Nonlinear Science and Numerical Simulation 15 (2010), no. 9, 2424-2430.

[6] T. A. Burton, Stability and periodic solutions of ordinary and functional differential equations. Corrected version of the 1985 original. Dover Publications, Inc., Mineola, NY, 2005.

[7] M.R. Zangooee, K. Hosseinzadeh, D. D. Ganji, Hydrothermal analysis of MHD nanofluid (TiO2-GO) flow between two radiative stretchable rotating disks using AGM. Case Studies in Thermal Engineering 14 (2019), 100460.

[8] M Gholinia, SAHK Moosavi, M Pourfallah, S Gholinia, DD Ganji, A numerical treatment of the TiO2/C2H6O2–H2O hybrid base nanofluid inside a porous cavity under the impact of shape factor in MHD flow. International Journal of Ambient Energy (2019), 1-8.

[9] S. S. Ghadikolaei, M Gholinia, ME Hoseini, D. D. Ganji, Natural convection MHD flow due to MoS2–Ag nanoparticles suspended in C2H6O2H2O hybrid base fluid with thermal radiation. Journal of the Taiwan Institute of Chemical Engineers 97 (2019), 12-23.

[10] M. Sheikholeslami, Numerical approach for MHD Al2O2-water nanofluid transportation inside a permeable medium using innovative computer method. Computer Methods in Applied Mechanics and Engineering 344 (2019), 306-318.

[11] K. Md. Rabbi, M. Sheikholeslami, A. Karim, A. Shafee, Z. L. Tliligh, Prediction of MHD flow and entropy generation by Artificial Neural Network in square cavity with heater-sink for nanomaterial. Physica A: Statistical Mechanics and its Applications 541 (2020), 123520.

[12] S. A. Shehzad, M. Sheikholeslami, T. Ambreen, A. Shafee, H. Babazadeh, Examination of CVFEM for nanofluid free convection MHD flow through permeable medium, 2020, https://doi.org/10.1007/s13204-020-01316-y.

[13] S. Kachapi, D.D. Ganji, A.G. Davodi, S.M. Varedi, Periodic solution for strongly nonlinear vibration systems by He's variational iteration method. Mathematical Methods in the Applied Sciences 32 (2009), no. 18, 2339-2349.

[14] A Asgari, D. D. Ganji, A. G. Davodi, Extended tanh method and exp-function method and its application to (2+ 1)-dimensional dispersive long wave nonlinear equations. Journal of the Applied Mathematics, Statistics and Informatics 6 (2010), no. 1, 61-72.

[15] D. D. Ganji, A. G Davodi, Y. A Geraily, New exact solutions for seventh-order Sawada-Kotera-Ito, Lax and Kaup-Kupershmidt equations using Exp-function method. Mathematical Methods in the Applied Sciences 33 (2010), no. 2, 167-176.

[16] S. S Ganji, G Domairry, A. G Davodi, H Babazadeh, S. H Seyedalizadeh Ganji, Higher-order approximations of motion of a nonlinear oscillator using the parameter expansion technique. International Journal of Modern Physics B 23 (2009), no.23, 4779-4789.

[17] D. D Ganji, M Babaelahi, A. A Joneidi, A.G. Davodi, Application of Exp-Function method to reduced Ostrovsky equation and Kuramoto-Sivashinsky equation. Asian-European Journal of Mathematics 2 (2009), no. 04, 567-578.

[18] G Domairry, Amin G Davodi, Arash G Davodi, Solutions for the double Sine-Gordon equation by Exp-function, Tanh, and extended Tanh methods. Numerical Methods for Partial Differential Equations 26 (2010), no. 2, 384-398.

[19] A Rajabi, J Alinejad, K Fallah, D. D. Ganji, Optimization of conjugate heat transfer in the electrofusion joint using Taguchi method. Thermal Science 23 (2019), no. 5 , 3047-3057.

[20] MR Shirkhani, A Hoshyar, DD Ganji, Application of VIM, HPM and CM to the system of strongly nonlinear fin problem. Journal of Engineering and Technology (JET) 9 (2018), no. 2, 1-13.

[21] Gao, Wei, Hadi Rezazadeh, Zehra Pinar, Haci Mehmet Baskonus, Shahzad Sarwar, and Gulnur Yel. Novel explicit solutions for the nonlinear Zoomeron equation by using newly extended direct algebraic technique. Optical and Quantum Electronics 52 (2020), no.1, 1-13.

[22] N. Raza, U. Afzal, A.R. Butt, H. Rezazadeh, Optical solitons in nematic liquid crystals with Kerr and parabolic law nonlinearities. Optical and Quantum Electronics 51 (2019), no. 1007, 1-16.

[23] H. Rezazadeh, A. Korkmaz, M. Eslami, S. M. Mirhosseini-Alizamini. A large family of optical solutions to Kundu-Eckhaus model by a new auxiliary equation method. Optical and Quantum Electronics 51 (2019), no. 84, 1-12.

[24] N. Raza, M. R. Aslam, H. Rezazadeh, .Analytical study of resonant optical solitons with variable coefficients in Kerr and non-Kerr law media. Optical and Quantum Electronics 59 (2019), no.51, 1-12.

[25] R. A.Talarposhti, Z. Asadi, H. Rezazadeh, D. D. Ganji, A. Bekir. Analytical solution for differential nonlinear and coupled equations in micropolar nanofluid flow between rotating parallel plates. The European Physical Journal Special Topics 228 (2019), no. 12, 2601-2617.

[26] J.H. He, Homotopy perturbation method for solving boundary value problems. Phys. Lett. A, 350 (2006), 87-88.

[27] J.H. He, Homotopy perturbation method: a new nonlinear analytical technique. Appl. Math. Comput, 135 (2003), 73-79.

[28] M. Shqair, Solution of different geometries reflected reactors neutron diffusion equation using the homotopy perturbation method. Results in Physics 12 (2019), 61-66.

[29] S. A. Pasha, Y. Nawaz, M. S. Arif, The modified homotopy perturbation method with an auxiliary term for the nonlinear oscillator with discontinuity. Journal of Low Frequency Noise 30 (2019), no. 3-4, 1363-1373.

[30] A. Aziz, S. Ray, F. Rahaman, B.K. Guha, Neutron star under homotopy perturbation method. Annals of Physics 409 (2019), 167918.

[31] M.J. Mahmoodabadi, Epidemic model analyzed via particle swarm optimization based homotopy perturbation method. Informatics in Medicine Unlocked 18 (2020) 100293

[32] S. Siddiqa, A. Faryad, N. Begum, M.A. Hossain, R. Subba, R. Gorla, Periodic magnetohydrodynamic natural convection flow of a micropolar fluid with radiation. International Journal of Thermal Sciences 111(2017), 215-222.

[33] D. Srinivasacharya, K. Hima Bindu, Entropy generation in a porous annulus due to micropolar fluid flow with slip and convective boundary conditions. Journal of Energy 111 (2016), 165-177.

[34] F. Mabood, S.M. Ibrahim, M.M. Rashidi, M.S. Shadloo, Giulio Lorenzini, Non-uniform heat source/sink and Soret effects on MHD non-Darcian convective flow past a stretchingsheet in a micropolar fluid with radiation. International Journal of Heat and Mass Transfer 93 (2016), 674-682.

[35] R. Ellahi, M. Hassan, A.Zeeshan, A. Khan, The shape effects of nanoparticles suspended in HFE-7100 over wedge with entropy generation and mixed convection. Appl. Nanosci, 6 (2016) 641-51.

[36] M. Akbarzadeh, S. Rashidi, M. Bovand, R. Ellahi, A sensitivity analysis on thermal and pumping power for the flow of nanofluid inside a wavy channel. Journal of Molecular Liquids 220 (2016) 1-13.

[37] R. Ellahi, M. Hassan, A.Zeeshan, A. Khan, Aggregation effects on water base Al2O3-nanofluid over permeable wedge in mixed convection. Asia-Pac. J. Chem. Eng. 11 (2016) 179-186.

[38] A.T. Akinshilo, A. Ilegbusi, H.M. Ali, A. Surajo, Heat transfer analysis of nanofluid flow with porous medium through Jeffery Hamel diverging/converging channel. Journal of Applied and Computational Mechanics 6 (2020), no. 3, 433-444.

[39] H.S Takhar, R. Bhargava, R.S. Agrawal, A. V.S. Balaji, Finite element solution of micropolar fluid flow and heat transfer between two porous disk. International Journal of Engineering Science 38 (2000) 1907-1922.

[40] M. Alizadeh, A.S. Dogonchi, D.D. Ganji, Micropolar nanofluid flow and heat transfer between penetrable walls in the presence of thermal radiation and magnetic field. Case Studies in Thermal Engineering 12 (2018), 319-332.

[41] Md. Alam, Nur, C.Tunç, An analytical method for solving exact solutions of the nonlinear Bogoyavlenskii equation and the nonlinear diffusive predator–prey system. Alexandria Engineering Journal. 11 (2016), no. 1, 152–161.

[42] Md Nur Alam, C. Tunç, Constructions of the optical solitons and others soliton to the conformable fractional Zakharov-Kuznetsov equation with power law nonlinearity. Journal of Taibah University for Science. 14 (2020), no.1, 94–100.

[43] Md. Nur Alam, C. Tunç, The new solitary wave structures for the (2+1)-dimensional time- fractional Schrodinger equation and the space-time nonlinear conformable fractional Bogoyavlenskii equations. Alexandria Engineering Journal. (2020) 59, 2221-2232.

[44] Md. Nur Alam, S. Aktar , C. Tunç, New solitary wave structures to the time fractional biological population. J. Math. Anal. 11 (2020), no. 3, 59–70.

[45] N. Shahid, C. Tunç, Resolution of coincident factors in altering the flow dynamics of an MHD elastoviscous fluid past an unbounded upright channel. Journal of Taibah University for Science 13 (2019), no.1, 1022-1034.

Author information

A.T. Akinshilo, Department of Mechanical Engineering, University of Lagos, Akoka- Yaba, Lagos, Nigeria.
E-mail: ta.akinshilo@gmail.com

A. G. Davodi, Department of Mechanical Engineering, Babol Noshirvani University of Technology, P.O. Box 484, Babol, Iran.
E-mail: a.g.davodi@gmail.com

H. Rezazadeh, Faculty of Engineering Technology, Amol University of Special Modern Technologies, Amol, Iran.
E-mail: rezazadehadi1363@gmail.com

G. Sobamowo, Department of Mechanical Engineering, University of Lagos, Akoka- Yaba, Lagos, Nigeria.
E-mail: mikegbeminiyi@gmail.com

Cemil Tunç, Department of Mathematics, Faculty of Sciences, Van Yuzuncu Yil University, 65080-Campus, Van, Turkey.
E-mail: cemtunc@yahoo.com

Received: November 07, 2020.
Accepted: February 21, 2021.